4-2011

Theoretical Investigation of a Reported Antibiotic from the 'Miracle Tree' Moringa Oleifera

Michael Horwath
University of Dayton

Vladimir Benin
University of Dayton, vbenin1@udayton.edu

Follow this and additional works at: https://ecommons.udayton.edu/chm_fac_pub

Part of the <u>Analytical Chemistry Commons</u>, <u>Biochemical Phenomena, Metabolism, and Nutrition Commons</u>, <u>Chemical and Pharmacologic Phenomena Commons</u>, <u>Environmental Chemistry Commons</u>, <u>Inorganic Chemistry Commons</u>, <u>Materials Chemistry Commons</u>, <u>Medical Biochemistry Commons</u>, <u>Medicinal-Pharmaceutical Chemistry Commons</u>, <u>Organic Chemistry Commons</u>, <u>Other Chemistry Commons</u>, and the <u>Physical Chemistry Commons</u>

Theoretical Investigation of a Reported Antibiotic from the "Miracle Tree" *Moringa oleifera*

Michael Horwath and Vladimir Benin*

Department of Chemistry

University of Dayton

*300 College Park*

Dayton, OH 45469-2357

Abstract

Moringa oleifera, sometimes called the "Miracle Tree," has received international attention for its potential to improve health in impoverished tropical areas. In addition to high vitamin content in the leaves and pods, the tree contains compounds with antioxidant and antibacterial properties. This study focused on the theoretical investigation of the suggested structure of one antibacterial compound, "pterygospermin," whose existence was proposed after some studies of the roots of *Moringa oleifera*. The structure of pterygospermin was first proposed by a research group working in the 1950s, but later studies have not found evidence of this compound and have instead attributed the antibacterial properties of *Moringa* to isothiocyanates. In order to investigate the possible existence and properties of pterygospermin, extensive *ab initio* and DFT calculations were conducted, to determine the most favorable isomer of pterygospermin and examine plausible decomposition pathways. This study concludes that pterygospermin, as proposed, would not be stable enough to exist in ambient conditions.

Introduction

The tree *Moringa oleifera* has recently received much international promotion in developing nations. It shows great promise as a dietary supplement in areas with minimal access to healthcare, due to both high vitamin content and documented antibacterial and anti-carcinogenic properties. However, there is still need for more definitive characterization of the chemistry of *Moringa,* to ensure that promotional efforts are based on firm data. Research can provide a critical link between natural pharmaceuticals such as *Moringa* and modern healthcare practices. This study has focused on one potential antibiotic compound from *Moringa,* "pterygospermin." The goal was to determine whether it is actually present in the tree roots and, if possible, provide characterization of its properties.
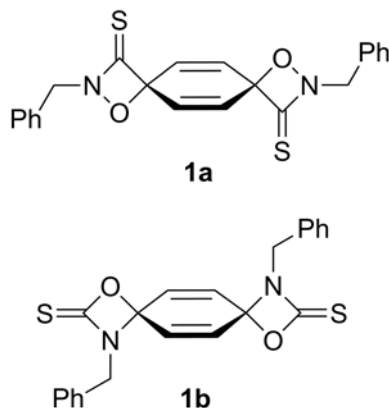
Much of the initial research on the chemistry of *Moringa* was conducted in India during the 1950s.[1-4] In the early 1950s, the research group of P. A. Kurup and P. L. Narasimha Rao reported extraction of pterygospermin from *Moringa* roots, as well as characterization of its bactericidal properties and structure.[2, 3] According to their studies, this compound was the major antibiotic component present in ethanol or benzene extractions. Lacking modern

instrumentation, such as NMR, they used chemical properties of pterygospermin to suggest two possible structural isomers **1a** and **1b**. The suggested structures were partially based on the observation that "pterygospermin" could decompose to produce another active compound, benzyl isothiocyanate, along with 1,4-benzoquinone (Scheme 1).


Scheme 1

1b
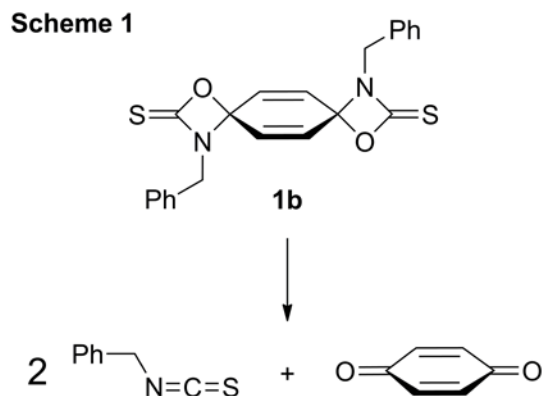
Pterygospermin was reported to have similar, but not identical, spectral properties to its decomposition product benzyl isothiocyanate, as well as slightly higher antibacterial potency. Although Kurup and Rao reported that pterygospermin was stable under ambient conditions, decomposition could readily occur under heat or acid conditions.

Later research worldwide, from the 1960s to the present, has added to knowledge of the anti-microbial and physiological activity of *Moringa* extracts, while providing a somewhat contrasting picture of the chemistry involved. Several studies point to isothiocyanates as the primary active compounds in *Moringa* seeds and roots, including benzyl isothiocyanate and 4-(α-L-rhamnosyloxy)benzyl isothiocyanate.[5, 6]

To investigate the theoretical possibility for existence and obtain an estimate on the stability (kinetic and thermodynamic) of the suggested pterygospermin structures, we conducted extensive *ab initio* and DFT calculations, with the following main objectives:

1) Optimize structures of **1a** and **1b**, including all stereoisomers, and determine the most energetically favorable structure.

2) Identify and optimize transition states for decomposition. Determine the theoretical stability and probable lifetime of pterygospermin.

3) Investigate thermal stability and decomposition of 1,3-oxazetidine-2-thione (**2**) and 1,2-oxazetidine-3-thione (**4**). These unusual four-membered rings are present in the suggested structures of pterygospermin, **1b** and **1a** respectively, and have previously received little attention in theoretical or synthetic studies.[7] However, the oxygen-containing analog of **2**, 1,3-oxazetinide-2-one (**3**), appears as an intermediate in certain synthetic procedures, and has been the subject of previous theoretical work.[8] The theoretical results on the decomposition of **2** and **4** are reported, and compared to the values previously reported for structure **3**.
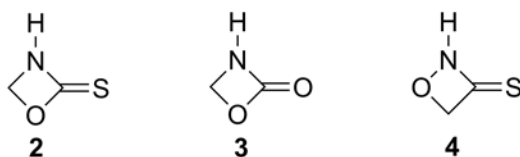
Results and Discussion

 Computational Protocol. All calculations were performed using the *Gaussian03/GaussView* software package[9] on a *Linux*-operated *QuantumCube QS4-2400C* by Parallel Quantum Solutions[10], or the *Gaussian03W/GaussViewW* package on a PC. Calculations were conducted at 298 K, and the primary model chemistry used was DFT at the *B3LYP/6-31+G(d)* level.[11-13] For the smaller model systems (**2**, **3** and **4**), calculations were also conducted at the *HF/6-31G(d), B3LYP/6-31G(d), MP2/6-31G(d), MP2/6-31+G(d)*, and *MP2/6-31++G(d,p)* levels of theory.

Stationary point searches were carried out using restricted singlet multiplicity. Several unrestricted-singlet and unrestricted-triplet calculations verified that restricted-singlet calculations provide the lowest energy for these systems. In addition, previously reported studies support the use of restricted calculations as a model for similar systems.[8] Transition state searches were conducted employing the Transit-Guided Quasi-Newton method (STQN, opt = qst2 or qst3)[14, 15] or the Berny algorithm (opt=ts). All minima and transition state structures were validated by subsequent frequency calculations at the same level of theory. Geometry minima had sets of only positive force constants, while transition states each had one imaginary frequency. Values of free energy changes were obtained after frequency calculations and zero-point energy corrections, and total energies (thermal plus electronic) were recorded from these calculations. ZPE scaling values were not considered necessary, because scaling factors for the level/basis sets used were close to unity. Thus, for *B3LYP/6-31G(d),* the primary level/basis used, the scale factor is 0.9806.[16] Also, the primary focus of this study was the difference in energies, which would be negligibly affected by the application of a scaling factor.

Relative Energies of Pterygospermin Isomers. Stationary points for a total of eight possible pterygospermin isomers/conformers were found at the *B3LYP/6-31+G(d)* level of theory. Two stereoisomers, **cis** and **trans**, were identified for each of the structural isomers, **1a** and **1b**, defined with regard to the orientation of the two four-membered rings relative to the central cyclohexadiene ring. In addition, two conformers were found for each stereoisomer, corresponding to the phenyl groups taking eclipsed or anti position (**syn** and **anti** conformer correspondingly). Ball-and-bond images of all eight optimized structures are shown in Figure 1, along with their relative Gibbs free energies. As evident from the data, within each set of isomers (**1a** or **1b**), the Gibbs free energy differences are quite small, especially in the case of the

1a isomers, whose values are all within less than 1 kcal/mol difference. Between the isomer sets, however, the energy difference is substantial, amounting to 77.6 kcal/mol, if the two most energetically favorable forms, **1a-trans-anti** and **1b-trans-anti**, are compared. The latter were used as starting geometries in the thermal decomposition studies.
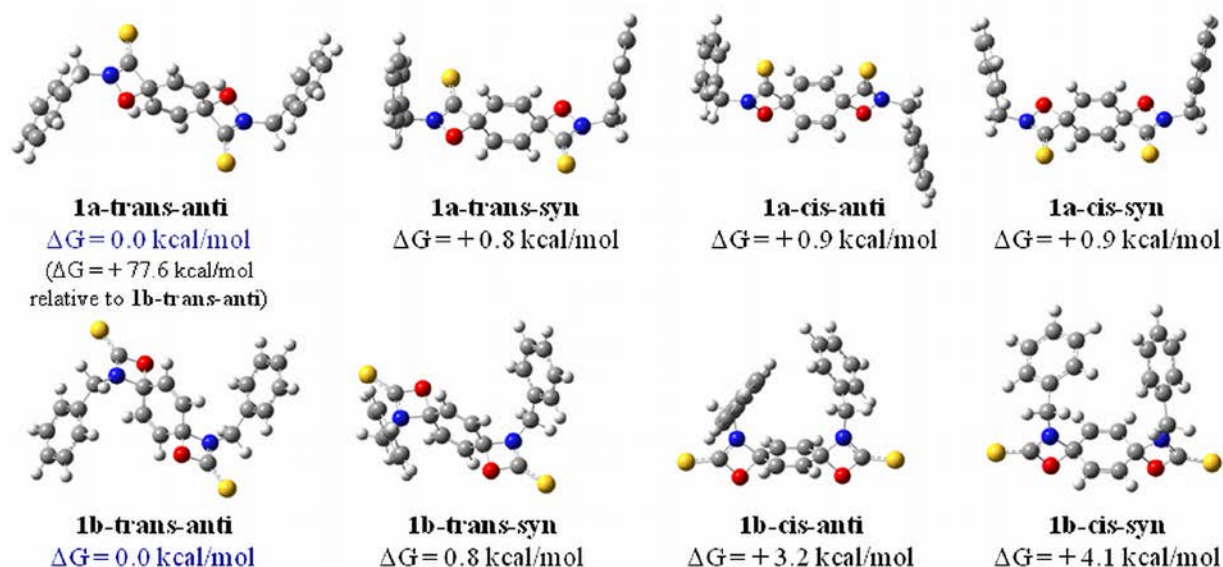

Figure 1. Ball-and-bond images of the stationary points of possible pterygospermin isomers/conformers, along with their relative Gibbs free energies. All structures and thermodynamic values from *B3LYP/6-31+G(d)* calculations.

Thermal Decomposition of Pterygospermin Isomers. We examined the thermal decomposition of the pterygospermin isomers **1a-trans-anti** and **1b-trans-anti**. In each of the cases two different modes of cleavage of the 4-membered rings were investigated, *Route 1* and *Route 2*. Each one of those was assumed to be a two-step process, corresponding to the sequential breaking of the two four-membered rings, as shown in Figures 2 and 3. As evident from the energy profiles, each step along *Route 1*, for both structures, is thermodynamically favorable, with relative Gibbs free energy values about -17 kcal/mol in the case of **1b** and roughly -55 kcal/mol for **1a**. Along the same route both pterygospermin isomers are predicted,

at this level of theory, to have significant kinetic barriers to decomposition, in the range of 30 – 40 kcal/mol, which would translate into very large half-life times at ambient temperature, amounting to more than 100 years. Clearly then, if *Route 1*, which corresponds precisely to the chemistry of decomposition suggested by Kurup and Rao, was the only available, then the proposed pterygospermin structures would indeed be expected to have sufficient thermal stability, in order to survive isolation and characterization.
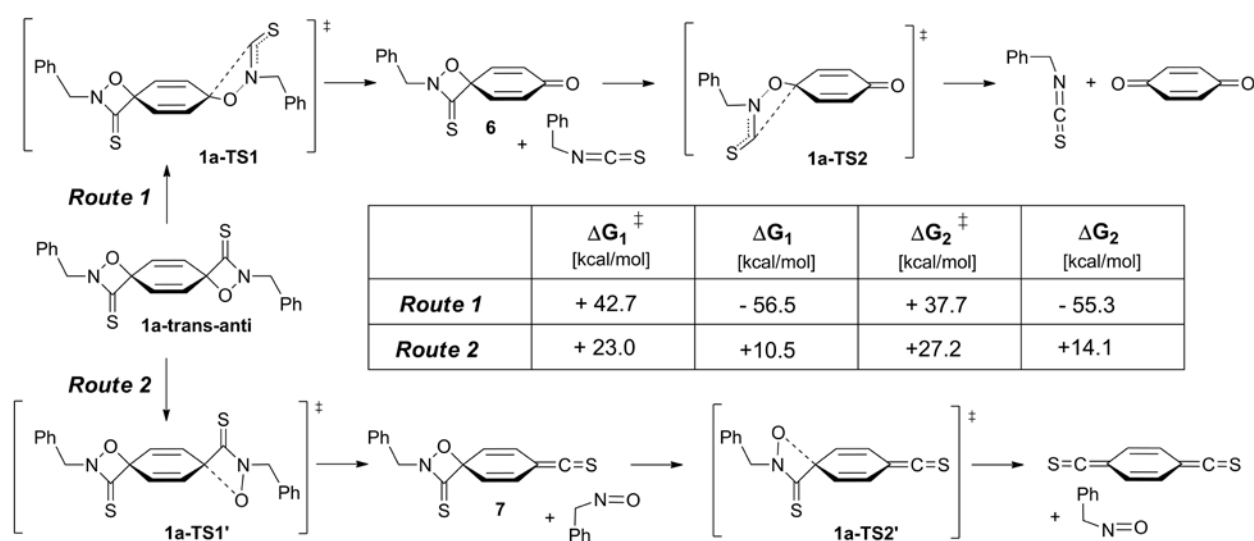

		$\Delta G_1^{\ddagger}$ [kcal/mol]	ΔG_1 [kcal/mol]	$\Delta G_2^{\ddagger}$ [kcal/mol]	ΔG_2 [kcal/mol]
	Route 1	+ 42.7	- 56.5	+ 37.7	- 55.3
	Route 2	+ 23.0	+10.5	+27.2	+14.1

Figure 2. Calculated Gibbs free energy reaction profiles of thermal decomposition of **1a-trans-anti**. *Route 1* results in the formation of benzylisothiocyanate. *Route 2* results in the formation of α-nitrosotoluene. All structures and thermodynamic values from *B3LYP/6-31+G(d)* calculations.

Figures 2 and 3 demonstrate, however, that for both suggested structures there is an alternative, and lower energy, pathway to decomposition, *Route 2*, which was never taken into account in the original studies. *Route 2* involves the breaking of the other pair of oppositely positioned bonds in the two four-membered rings. For structure **1a-trans-anti** the individual steps are not as thermodynamically favorable, and are in fact both endothermic. However, the activation barriers are substantially lower compared to those along *Route 1*, by at least 10 and even 15 kcal/mol. In

the case of **1b-trans-anti**, both reaction free energies are significantly more favorable, and the barriers of activation are much lower, in comparison to values along *Route 1*. Along *Route 2*, half-life times are reduced to about 2.5 h for **1a-trans-anti** and 2 seconds for **1b-trans-anti**. Clearly, in either case not fitting a compound which was suggested to accumulate and be isolable from parts of the *Moringa* tree.
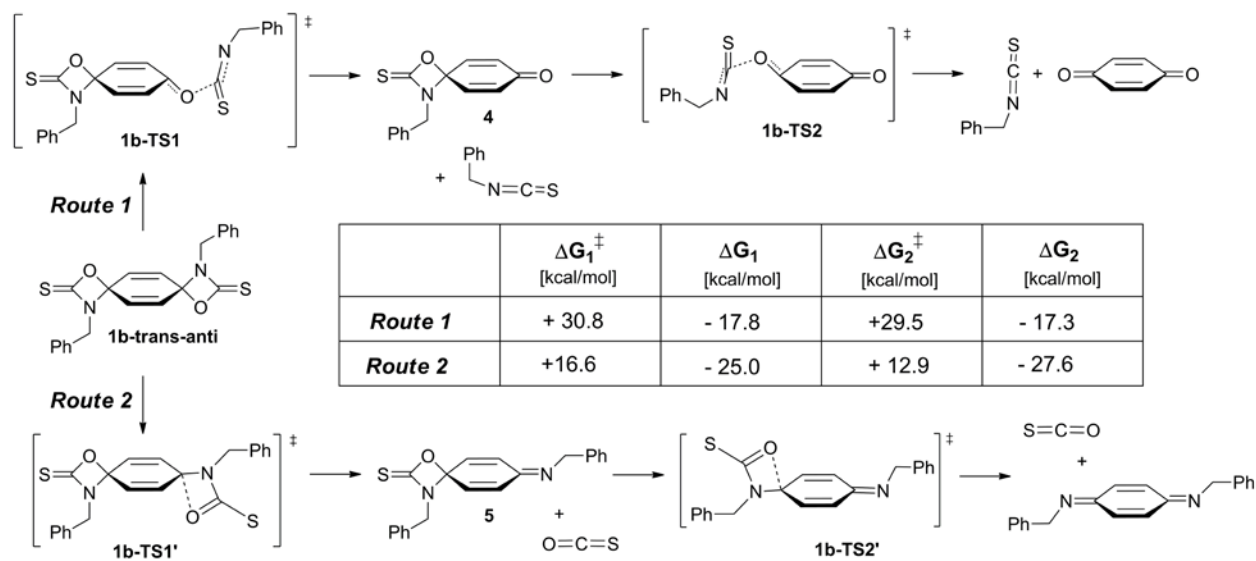

	$\Delta G_1^{\ddagger}$ [kcal/mol]	ΔG_1 [kcal/mol]	$\Delta G_2^{\ddagger}$ [kcal/mol]	ΔG_2 [kcal/mol]
Route 1	+ 30.8	- 17.8	+29.5	- 17.3
Route 2	+16.6	- 25.0	+ 12.9	- 27.6

Figure 3. Calculated Gibbs free energy reaction profiles of thermal decomposition of **1b-trans-anti**. *Route 1* results in the formation of benzylisothiocyanate. *Route 2* results in the formation of carbonyl sulfide (COS). All structures and thermodynamic values from *B3LYP/6-31+G(d)* calculations.

Regardless of the followed route, each elementary step is concerted and involves the breaking of two bonds, oppositely positioned in the four-membered ring. The bond breaking, albeit it concerted, is notably asynchronous, with one of the bond breaking events occurring to a much greater extent at the TS, as shown for structure **1b-trans-anti** in Figure 4. In every case it is the breaking of the bond to the carbon of the central six-membered ring, likely related to the latter's ability to interact favorably with the conjugated double bonds of the central ring. In the absence of such environment, as in structures **2** and **4**, the transition state structures for the breaking of

the four-membered rings show a much more symmetrical pattern, with comparable degrees of bond-breaking of both bonds undergoing cleavage (*vide infra*).
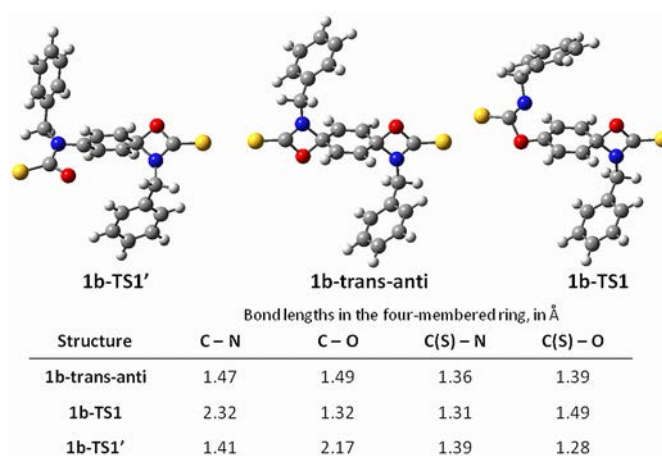

Structure	C – N	C – O	C(S) – N	C(S) – O
1b-trans-anti	1.47	1.49	1.36	1.39
1b-TS1	2.32	1.32	1.31	1.49
1b-TS1′	1.41	2.17	1.39	1.28

Figure 4. Comparative geometries and structural parameters of **1b-trans-anti**, **1b-TS1** and **1b-TS1'**. Structures and bond lengths from *B3LYP/6-31+G(d)* calculations.

Thermal decomposition of 1,3-oxazetidine-2-thione (2) and 1,2-oxazetidine-3-thione (4). The 4-membered rings of structures **2** and **4** were used as minimal models, to further investigate the decomposition of pterygospermin isomers **1a** and **1b**. Figure 5 shows the decomposition routes for compounds **2** and **4**, with cleavage, in each case, of one or the other pair of opposite bonds in the four-membered ring. Principal calculations were conducted at the *B3LYP/6-31+G(d)* level. Additionally, for structure **2**, calculations were also carried out at the *HF/6-31G(d), B3LYP/6-31G(d)*, *MP2/6-31G(d), MP2/6-31G+(d)*, and *MP2/6-31G++(d,p)* levels, with results reported in Table 1. The highest computed barrier in each case is obtained at the *HF/6-31G(d)* level. Some reduction of the barrier is observed upon introduction of diffuse functions, both for the DFT and the MP2 calculations.
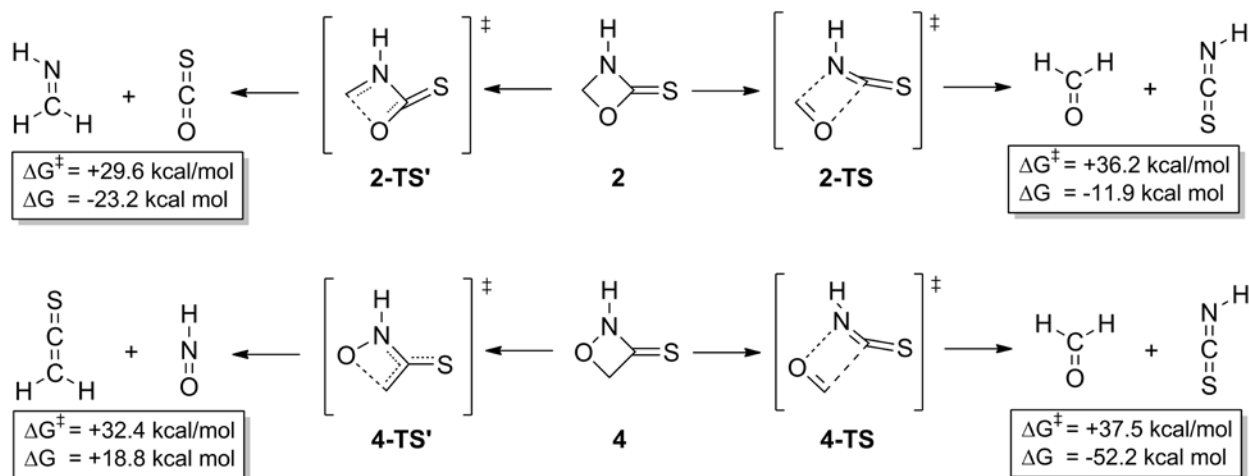
Figure 5. Calculated Gibbs free energy reaction profiles of thermal decomposition of 1,3-oxazetidine-2-thione (**2**) and 1,2-oxazetidine-3-thione (**4**). All structures and thermodynamic values from *B3LYP/6-31+G(d)* calculations.

As the results from Table 1 clearly show, with any of the used methods/levels of theory, the second route to decomposition, with generation of carbonyl sulfide (CSO) + methyleneimine, has a lower barrier. However, the difference in relative Gibbs free energies between **2-TS** and **2-TS′** varies. Thus, the difference is roughly 10 kcal/mol, if using HF/6-31G(d) and about 7 kcal/mol if B3LYP is used (largely invariant with basis set). The gap is considerably narrower in MP2 calculations, especially with the 6-31+G(d) or the 6-31++G(d,p) basis set, when it is only about 2 kcal/mol.

Table 1. Values of activation and thermodynamic parameters in the thermal decomposition of 1,3-oxazetidine-2-thione (Compound **2**, Scheme 2) using several methods and levels of theory. Energy values in kcal/mol.

Method	Basis Set	Decomposition to H_2CO + HNCS (*via* **2-TS**)		Decomposition to CSO + CH_2=NH (*via* **2-TS′**)	
		ΔG_{298}	$\Delta G^{\neq}_{298}$	ΔG_{298}	$\Delta G^{\neq}_{298}$
HF	*6-31G(d)*	-13.1	51.6	-25.7	42.0
B3LYP	*6-31G(d)*	-10.9	38.3	-21.8	30.9
B3LYP	*6-31+G(d)*	-11.9	36.2	-23.2	29.6
MP2	*6-31G(d)*	-13.1	41.2	-25.9	37.3
MP2	*6-31+G(d)*	-12.7	37.4	-27.2	34.9
MP2	*6-31++G(d,p)*	-12.6	37.0	-27.2	35.1

Examination of TS geometries reveals significant contrast between the transition states **2-TS/4-TS,** and their counterparts in the decomposition of **1b-trans-anti** or **1a-trans-anti,** correspondingly.   As mentioned above, all transition states for decomposition of **1a/1b** are considerably asymmetrical, with much greater relative lengthening of the bond between the heteroatom (N or O) and the carbon from the central six-membered ring. The transition states **2-TS** and **4-TS**, on the other hand, exhibit a much more symmetrical pattern, as shown in Figure 6. The asymmetrical pattern is still observed, however, in the cases of **2-TS′** and **4-TS′**.

Structure	C − N	C − O	C(S) − N	C(S) − O
2	1.46	1.45	1.38	1.39
2-TS	1.78	1.29	1.28	2.08
2-TS′	1.35	2.06	1.46	1.27

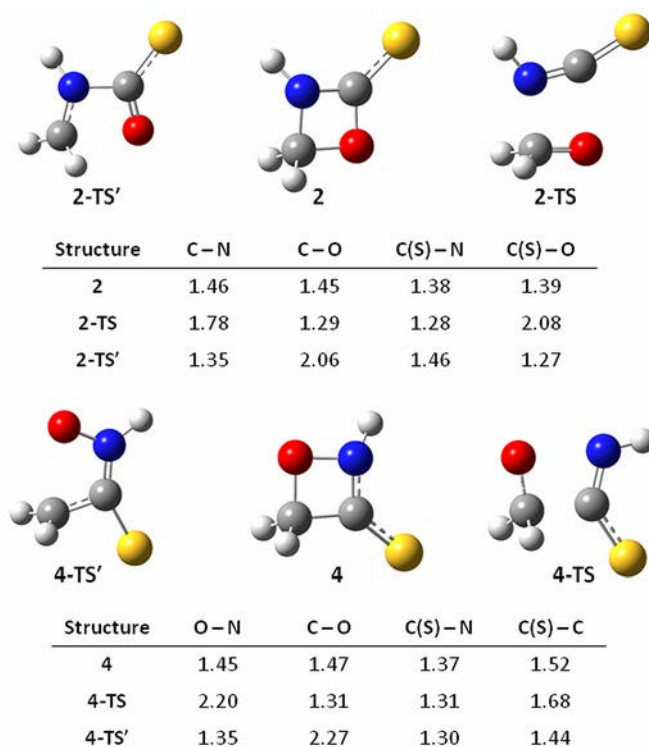| Structure	O − N	C − O	C(S) − N	C(S) − C
4	1.45	1.47	1.37	1.52
4-TS	2.20	1.31	1.31	1.68
4-TS′	1.35	2.27	1.30	1.44

Figure 6. <u>Top row:</u> Comparative geometries and bond lengths (in Å) of 1,3-oxazetidine-2-thione (**2**) and the transition states to its decomposition (**2-TS** and **2-TS′**); <u>Bottom row:</u> Comparative geometries and bond lengths (in Å) of 1,2-oxazetidine-3-thione (**4**) and the transition states to its decomposition (**4-TS** and **4-TS′**). Structures and bond lengths from *B3LYP/6-31+G(d)* calculations.

11

*Comparative study of the thermal decomposition of 1,3-oxazetidine-2-thione (**2**) and 1,3-oxazetidine-2-one (**3**).* Previous reports of compounds closely matching the 4-membered ring structure of pterygospermin are lacking in both synthetic and theoretical literature. However, the related structure 1,3-oxazetinide-2-one (**3**) has been suggested as an intermediate in the cycloaddition reaction of an isocyanate and a ketone to form an imine. De-Cai Fang and Xiao-Yuan Fu performed a detailed computational study of the kinetics of formation of 1,3-oxazetidine during this process, including consideration of a variety of substituents on the isocyanate and ketone.[8] The reaction scheme for the non-substituted case closely matches the reverse of the decomposition of structure **2** (Scheme 3).

Scheme 3
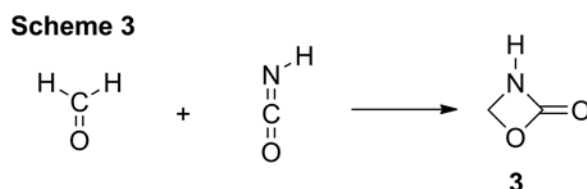
In accordance with the Principle of Microscopic Reversibility, the transition state should remain the same for the backward (decomposition) direction of the reaction path. Thus, energy values, reported by De-Cai Fang and Fu for the formation of **3,** could be used to determine ΔG_{298} and $\Delta G^{\ddagger}_{298}$ for its decomposition, and were used for comparison with structure **2**. The results are shown in Table 2. The activation barriers to decomposition of both **2** and **3** exhibit significant decrease with change of method from HF to MP2, keeping the same basis set. Further barrier reduction is observed upon increase of the basis set. The relative heights of the energy barriers also change. At the HF level the activation barrier for **3** is somewhat smaller than that for **2** but it is opposite at the MP2 level, with increasing difference when using a more extensive basis set.

Table 2. Comparison of the activation and thermodynamic parameters in the thermal decompositions of 1,3-oxazetidine-2-thione (**2**) and 1,3-oxazetidine-2-one (**3**).

Structure	Method	Basis Set	$\Delta G_{298}{}^{a}$ [kcal/mol]	$\Delta G^{\neq}{}_{298}$ [kcal/mol]
2	HF	*6-31G(d)*	-13.1	51.6
2	MP2	*6-31G(d)*	-13.2	41.1
2	MP2	*6-31++G(d,p)*	-12.6	37.0
3	HF	*6-31G(d)*	-7.6	49.3
3	MP2	*6-31G(d)*	-3.1	42.4
3	MP2	*6-31++G(d,p)*	-6.8	40.8

[a] Calculated as the difference between the Gibbs free energy of the initial structure (**2** or **3**) and the sum of the Gibbs free energies of the products of decomposition.

Conclusions

The most important results from this computational study can be summarized as follows:

1) The pterygospermin structures **1a-b**, suggested by Kurup and Rao, are not viable with regard to isolation, storage and characterization. The pathway to decomposition matching the one originally proposed by Kurup and Rao has been identified computationally, and the activation barriers are indeed high enough to allow for kinetically stable structures. However, for each of the suggested structures a lower-energy route has been identified, leading to half-life times in the order of seconds to a couple of hours. Thus, calculations seem to rule out the possibility for a long-term storage and isolation/characterization of those structures.

2) Although not part of this report, extraction/chromatography studies conducted recently in our laboratory have consistently identified benzyl isothiocyanate among the extracted components, but have failed to identify *p*-benzoquinone, even though it is a terminal molecule in the decomposition of either **1a** or **1b**, following the scheme proposed by

Kurup and Rao. This too is inconsistent with the presence of pterygospermin, even as a metastable structure.

3) Unlike structures **1a-b**, the parent four-membered rings, **2** and **4**, exhibit much higher computed barriers to decomposition, making them reasonable targets for preparation and characterization. Our experimental efforts are currently focused on achieving this goal.

4) This study also demonstrates the limit of possible simplification in the investigation of the pterygospermin system. Although decomposition affects primarily the four-membered ring structure, it is somewhat misleading to use structures **2** or **4** as reliable model systems. Values of $\Delta G^{\neq}_{298}$ for the pterygospermin isomers **1a-b** are significantly lower compared to those of **2** or **4** at the same level/basis set. Also, transition state geometries are notably different. Thus, caution must be exercised when considering results from over-simplified models.

Supporting Information Available. Energies and thermodynamic parameters of all stationary points are summarized in the Supplementary Materials, Tables S1 – S11.

References

* Corresponding author. Phone: 937-229-4762; Fax: 937-229-2635; E-mail: vladimir.benin@notes.udayton.edu

[1] G.S. Chatterjee, S.R. Maitra, Science and Culture, 17 (1951), 43 - 44.

[2]   P.A. Kurup, P.L.N. Rao, J. Ind. Inst. Sci., 34a (1952), 219 - 227.

[3]   P.A. Kurup, P.L.N. Rao, Ind. J. Med. Res., 42 (1954), 85 - 95.

[4]   R.R. Rao, M. George, Ind. J. Med. Res., 37 (1949), 159 - 167.

[5]   U. Eilert, B. Wolters, A. Nahrstedt, J. Med. Plant Res., 42 (1981), 55 - 61.

[6]   D. Gueyrard, in: A.P. Rauter (Ed.), Natural Products in the New Millenium: Prospects and Industrial Application, Kluwer Academic, Dordrecht, 2002, pp. 415 - 419.

[7]   P.V. Sudhakar, J. Chandrasekhar, J. Mol. Struct., 194 (1989), 135 - 147.

[8]   D. Fang, X. Fu, J. Mol. Struct. (THEOCHEM), 459 (1999), 15 - 21.

[9]   R.C. Gaussian 03, Frisch, M. J.; Trucks, G. W.; Schlegel, H. B.; Scuseria, G. E.; Robb, M. A.; Cheeseman, J. R.; Montgomery, Jr., J. A.; Vreven, T.; Kudin, K. N.; Burant, J. C.; Millam, J. M.; Iyengar, S. S.; Tomasi, J.; Barone, V.; Mennucci, B.; Cossi, M.; Scalmani, G.; Rega, N.; Petersson, G. A.; Nakatsuji, H.; Hada, M.; Ehara, M.; Toyota, K.; Fukuda, R.; Hasegawa, J.; Ishida, M.; Nakajima, T.; Honda, Y.; Kitao, O.; Nakai, H.; Klene, M.; Li, X.; Knox, J. E.; Hratchian, H. P.; Cross, J. B.; Bakken, V.; Adamo, C.; Jaramillo, J.; Gomperts, R.; Stratmann, R. E.; Yazyev, O.; Austin, A. J.; Cammi, R.; Pomelli, C.; Ochterski, J. W.; Ayala, P. Y.; Morokuma, K.; Voth, G. A.; Salvador, P.; Dannenberg, J. J.; Zakrzewski, V. G.; Dapprich, S.; Daniels, A. D.; Strain, M. C.; Farkas, O.; Malick, D. K.; Rabuck, A. D.; Raghavachari, K.; Foresman, J. B.; Ortiz, J. V.; Cui, Q.; Baboul, A. G.; Clifford, S.; Cioslowski, J.; Stefanov, B. B.; Liu, G.; Liashenko, A.; Piskorz, P.; Komaromi, I.; Martin, R. L.; Fox, D. J.; Keith, T.; Al-Laham, M. A.; Peng, C. Y.; Nanayakkara, A.; Challacombe, M.; Gill, P. M. W.; Johnson, B.; Chen, W.; Wong, M. W.; Gonzalez, C.; and Pople, J. A.; Gaussian, Inc., Wallingford CT, 2004.

[10]   *Parallel Quantum Solutions*, 2013 Green Acres Road, Suite A, Fayetteville, Arkansas 72703.

[11]   A.D. Becke, Phys. Rev. A, 38 (1988), 3098 - 3100.

[12]   M.J. Frisch, J.A. Pople, J.S. Binkley, J. Chem. Phys., 80 (1984), 3265 - 3269.

[13]   C. Lee, W. Yang, R.G. Parr, Phys. Rev. B, 37 (1988), 785 - 789.

[14]   C. Peng, P.Y. Ayala, H.B. Schlegel, M.J. Frisch, J. Comp. Chem., 17 (1996), 49.

[15]   C. Peng, H.B. Schlegel, Israel J. Chem., 33 (1994), 449.

[16]   J. Zheng, B.J. Lynch, Y. Zhao, D.J. Truhlar, Database of Frequency Scaling Factors for Electronic Structure Methods, 2009.